ICARUS **120,** 87–105 (1996)
ARTICLE NO. 0039

Ejecta Blocks on 243 Ida and on Other Asteroids

PASCAL LEE, JOSEPH VEVERKA, PETER C. THOMAS, AND PAUL HELFENSTEIN

Center for Radiophysics and Space Research, Cornell University, Ithaca, New York 14853-6801
E-mail: lee@astrosun.tn.cornell.edu

MICHAEL J. S. BELTON

National Optical Astronomy Observatories, Tucson, Arizona 85719

CLARK R. CHAPMAN

Planetary Science Institute, Tucson, Arizona 85719

RONALD GREELEY, ROBERT T. PAPPALARDO, AND ROBERT SULLIVAN

Department of Geology, Arizona State University, Tempe, Arizona 85287-1404

AND

JAMES W. HEAD, III

Geological Sciences Department, Brown University, Providence, Rhode Island 02912

Received March 31, 1995; revised August 29, 1995

Seventeen positive relief features ~45–150 m across are identified as probable blocks in Galileo high-resolution images of Ida. Their presence provides direct evidence for regolith retention on asteroids. The spatial distribution, maximum size, and integrated volume of the blocks are consistent with those of blocks associated with craters on the Earth, the Moon, Phobos, and Deimos. The concordance suggests that the features are impact ejecta fragments and that cratering mechanics on Ida, an object of average diameter ~32 km, are similar to those applying on previously studied rocky bodies. The blocks that lie within or near the rims of craters Lascaux and Mammoth were likely mobilized in the low-velocity tail portion of the excavation flow that formed those craters. A few blocks located near smaller craters may have migrated some distance away from their source, possibly by impact-induced spallation, hopping, rolling, and/or sliding. Some blocks on Ida could be surviving fragments from the Koronis parent body, accreted after its breakup. The lifetime of 10^2-m sized boulders against collisional disruption is estimated to be in the 10^8–10^9 year range, consistent with ages considered for the largest and oldest craters on Ida. Extrapolation of successful ejecta scaling laws to other asteroids suggests that blocks ~15 and 70 m across could be present on Dactyl and Gaspra, respectively (in both cases too small to be identified in available Galileo images). Blocks 100 m in size could be present on 433 Eros, and km-sized megablocks on 4 Vesta.

1. INTRODUCTION AND SUMMARY

The recent flybys of 243 Ida and 951 Gaspra by the Galileo spacecraft yielded the first high-resolution images of the surfaces of main belt asteroids, providing a unique opportunity to study the geological evolution of these small bodies, in particular their collisional history. Of special interest has been the discovery on Ida of discrete positive relief features (PRFs) identified as probable blocks (Belton *et al.* 1994, Chapman *et al.* 1994a). The features appear as localized topographic highs, typically several tens of meters across, casting distinct shadows. More PRFs that are possible blocks also are visible on Ida and some are seen on Gaspra. However, the available resolution, viewing conditions, and/or roughness of the background topography make their identification less definitive (e.g., P. Lee *et al.* 1994).

Blocks have been observed before on small bodies, namely on Phobos and Deimos, where their origin was linked to the largest and/or freshest impact craters (Thomas 1979, S. Lee *et al.* 1986). The blocks on the martian satellites are believed to be coherent ejecta fragments like those found in association with impact structures on the Earth and on the Moon. Until the receipt of Galileo images, however, it remained unclear whether such ejecta blocks or any regolith cover would also exist on asteroids

0019-1035/96 $18.00

of similar size ($<10^2$ km across). One possibility was that Phobos and Deimos have retained a significant regolith because the satellites orbit relatively deep in the gravitational well of Mars (Soter 1971). Earth-based polarimetric, radiometric, and thermal observations (e.g., Dollfus *et al.* 1989, Lebofsky and Spencer 1989), the meteoritic record (e.g., Bunch and Rajan 1989), and theoretical modeling (e.g., Housen *et al.* 1979, Asphaug and Melosh 1993) indicate that some asteroids possess regoliths, but *in situ* visual evidence of regolith components was lacking until the Galileo flybys.

The existence of blocks on Ida is interesting for several reasons. The features represent the coarsest fraction of a regolith, and as such, are direct evidence of regolith retention on asteroids. They provide information on the physical properties and processing history of asteroid surfaces, and offer insight into the internal structure of asteroids by helping constrain material strength. Moreover, as retained ejecta fragments, they provide information on the impact cratering process on bodies with low gravity, small radius of curvature, and relatively fast rate of spin, free from the strong gravitational influence of any nearby planet that could allow the recovery of escaping ejecta (e.g., Cintala *et al.* 1978, 1979). Insight into the generation of meteoroids may also be gained through a better understanding of the block production process on asteroids.

In this paper, we examine the features that are readily identifiable as blocks on Ida (Section 2). We begin with a description of the blocks, assess their spatial distribution, discuss the effects of observational biases on their mapping, and determine block and crater densities for two localities (Section 2.1). We show that most blocks lie within or near the rims of relatively large impact craters (Lascaux and Mammoth) and that, to first order, there is an apparent anticorrelation between block surface density and crater density. We next examine the size distribution of the blocks (Section 2.2) and compare block volumes to the total volume of material ejected from craters (Section 2.3). We show that the dimensions of the largest blocks found on Ida are consistent with the maximum fragment size predicted by empirical scaling laws established for ejecta blockfields on the Earth, the Moon, Phobos, and Deimos. Next follows a discussion on the origin of the blocks in which various modes of emplacement are examined (Section 2.4). We show that the available data, ejecta scaling laws, results from hydrocode modeling and the expected lifetimes of blocks against collisional disruption are consistent with the blocks at Lascaux and Mammoth having originated from those structures. We emphasize, however, that other block emplacement mechanisms, such as the asymmetric rotational sweep-up of suborbitally launched blocks proposed by Geissler *et al.* (1994, 1995, 1996) or the migration of blocks into lows in dynamic height may have contributed to the observed block distribution. Some blocks might also be surviving fragments from the Koronis parent body. We continue with a brief discussion on the possibility of blocks on Dactyl and Gaspra, and show that the largest blocks normally expected on these objects would not be adequately resolved in the available Galileo images (Section 3). We also speculate on maximum block sizes on other asteroids, and find that hundred-meter-sized fragments might be present on 433 Eros, while km-sized megablocks could occur 4 Vesta.

2. BLOCKS ON 243 IDA

2.1. Spatial Distribution

Seventeen PRFs are readily identified as blocks in high-resolution images of Ida (31–38 m/pixel) (Fig. 1 and Table I). The features range in size from ~150 m down to ~45 m. From the length of their shadows, the larger ones (blocks no. 1 and 14) appear to be about half as high as they are wide. Such aspect ratios suggest a stable configuration, although this remains difficult to ascertain as local slopes are poorly known and block outlines are ill-resolved. Moreover, partial burial of blocks is possible. Several blocks (within crater Mammoth) appear to lie atop broad rises, somewhat reminiscent of the basal debris aprons surrounding older ejecta blocks on the Moon. Block positions (line and sample coordinates) listed in Table I were determined by selecting the starkest contrast (steepest gradient in density number [DN]) between two adjacent pixels at a block's location and by recording the line and sample of the brightest pixel in the pair. Figs. 2 and 3 show a series of images and a stereo pair in which the blocks are visible.

The spatial distribution of the blocks is non-uniform, with distinct clusters in the eastern region of Ida (Pola Regio) and in the most distal portion of the western region (area of Palisa Regio near Vienna Regio) (Fig. 1). Of the 13 blocks in the eastern region, 12 lie within or near the rims of craters Lascaux and Mammoth, two 11-km diameter impact structures, the largest integral craters in the ''hemisphere'' of Ida covered in the high-resolution mosaic. Of the 4 blocks in the western region, 2 are located within or on the rim of a smaller impact structure, the 2.2-km diameter crater Padirac. No blocks are readily identifiable along most of Ida's limb nor in the central portion of the mosaic shown in Fig. 1 (most of Palisa Regio).

Several factors affect the mapping of blocks, one of which is photometric geometry. In Lunar Orbiter images of the Moon, blocks associated with impact craters are more easily seen where the incidence angle, i, is large (away from the sun-facing portions of crater walls and rims) and where the emission angle, e, is relatively small (Schultz 1976). The absence of readily identifiable blocks along most of Ida's limb is not surprising: limb observations are impaired by significant foreshortening (large e) and, in the case of the Ida mosaic which shows the asteroid at a phase

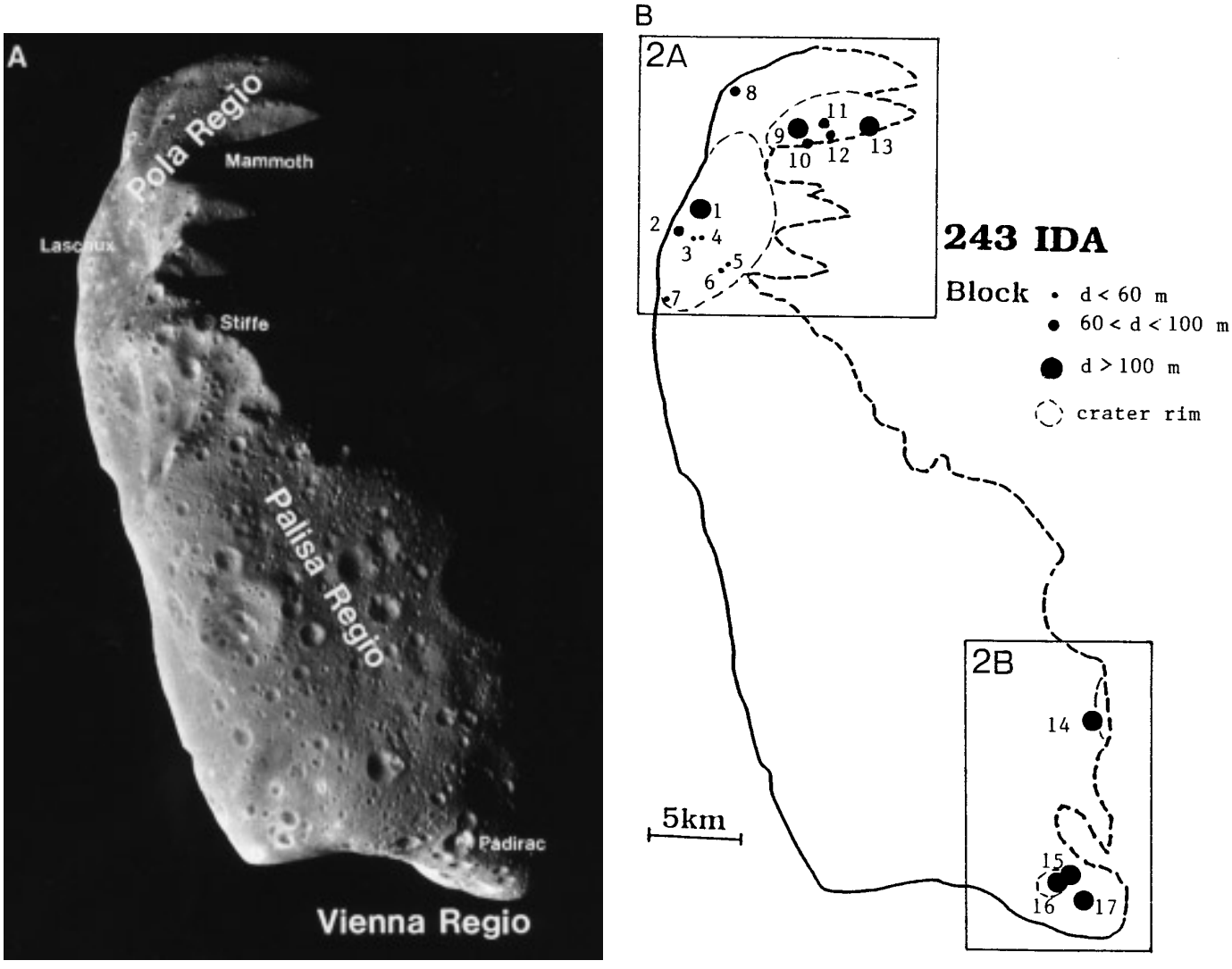

FIG. 1. (A) Galileo high-resolution mosaic of Ida; (B) Map of blocks, Boxes 2A and 2B delineate the areas shown in Figs. 2A and 2B, respectively.

angle of ~50°, also by unfavorable illumination (small i). A single, very high-resolution image (202562778: 24 m/pixel, phase angle $\alpha = 109°$) was also acquired by the Galileo SSI instrument. Considered alone, the improved spatial resolution would allow any block larger than a few tens of meters across to be identified in this image were it present. No block is readily seen, however, except for a marginal candidate near the bottom of crater Stiffe. Because high phase angle and significant foreshortening of the illuminated terrains can mitigate the benefit of improved spatial resolution, no reliable conclusion as to the presence or absence of blocks less than ~3 pixels high (with corresponding widths ~6 pixels across) can be reached for image 202562778. As for well-exposed blocks more than ~6 pixels high (≥150 m), their absence is quite definitive.

Block mapping over the high-resolution mosaic is also affected by variations in spatial resolution and in the availability of stereo coverage. The eastern region was viewed at the highest resolution available (31 m/pixel) and with substantial stereo coverage (Fig. 3). Blocks only ~45 m in size (<2 pixels across) could be identified here. In contrast, the western region was viewed at a resolution of only 38 m/pixel and with almost no stereo coverage. No block smaller than ~130 m (~3.5 pixels across) is recognizable there. Blocks appear to be altogether absent in the central portion of the asteroid. The central region was viewed at an intermediate resolution of ~34 m/pixel and under geometries that would have allowed large blocks such as those in the western region to be identified were they present. Moreover, smearing is not significant, foreshortening is minimal, and incidence angles are sufficiently large (Fig. 4). An explanation for the lack of blocks in the central

TABLE I
Blocks on Ida

Block Number	Image Number	Line	Sample	Lat.*	Lon.*	Block Size (m)
1	202562439	581	199	3.3°N	172.4°	130
	202562339	74	320			
2	202562439	616	157	9.2°N	172.7°	90
	202562339	112	283			
3	202562439	632	181	6.0°N	170.7°	45
	202562339	117	310			
4	202562439	634	196	4.1°N	170.0°	45
	202562339	118	323			
5	202562439	706	239	12.2°S	149.6°	45
	202562339	167	372			
6	202562439	712	222	0.2°S	162.7°	45
	202562339	176	354			
7	202562439	761	119	16.8°N	165.6°	45
	202562339	237	260			
8	202562439	349	283	2.8°S	182.0°	70
9	202562439	447	381	13.3°S	178.8°	130
10	202562439	479	391	14.8°S	177.9°	90
11	202562439	445	422	15.4°S	181.0°	70
12	202562439	473	434	16.7°S	180.7°	90
13	202562439	475	500	19.7°S	185.0°	150
14	202562313	179	477	24.8°S	2.8°	150
15	202562313	418	442	5.9°S	3.8°	130
16	202562313	430	430	4.5°S	4.3°	130
17	202562313	456	468	3.3°S	359.2°	130

* I.A.U. convention: 243 Ida's rotation is retrograde; longitudes increase towards the east. The regions designated ''eastern,'' ''central'' and ''western'' in the text (see also Figures 1 and 6) are at longitudes ~180°, ~90°, and ~0°, respectively. Block latitudes and longitudes are approximate due to uncertainties in the shape model. They were averaged between images where applicable. The spatial resolutions of images 202562439, 202562339 and 202562313 are 31, 34 and 38 m/pixel, respectively.

region might be provided by terrain roughness. The background topography in this region is distinctly rougher than elsewhere, making isolated blocks more difficult to identify. The four blocks in the western region do occur over topography about as rough as that characterizing the central portion of Ida, but the sizes of those blocks are among the largest found. Thus, while no definitive conclusion can be reached with regard to the abundance of small blocks, a case can be made for a true dearth in large blocks in the central region: in comparison with the western region and even more so with the eastern region, the central portion of Ida appears lacking in blocks larger than ~3.5 pixels across, i.e., >120 m across. We offer a possible explanation for this scarcity in Section 2.4.5.

The distribution of blocks on Ida can be compared usefully to regional differences in crater density (Belton *et al.* 1994). In the present study, we examine two localities: (i) the densely cratered central region (Palisa Regio), and (ii) the sparsely cratered interiors of large craters in the eastern region (craters Lascaux and Mammoth) (Figs. 1A and 5). Taking into account only craters ≥0.5 km and <10 km in diameter, Palisa Regio has a cumulative density of ~0.30 crater · km^{-2}, whereas the interiors of Lascaux and Mammoth have densities of ~0.05 crater · km^{-2}, after correction for the partial viewing of those craters. Counting only blocks ≥60 m across to minimize any resolution bias, we find block surface densities of $d \leq 0.01$ block · km^{-2} over Palisa Regio and $d \sim 0.03$ block · km^{-2} inside Lascaux and Mammoth. Thus, there appears to be an anticorrelation between the surface density of blocks and crater density: most identifiable blocks ≥60 m across occur over the sparsely cratered interiors of the large eastern craters. An interpretation of this anticorrelation is offered in Section 2.4.5.

FIG. 2. (A) Image 202562439 showing the 11-km diameter craters Lascaux and Mammoth in the eastern region and 13 blocks. Resolution is 31 m/pixel. (B) Portion of image 202562313 showing the 4 blocks in the western region, two of which lie on the walls of crater Padirac. Resolution is 38 m/pixel. Scale bars are 5 km long.

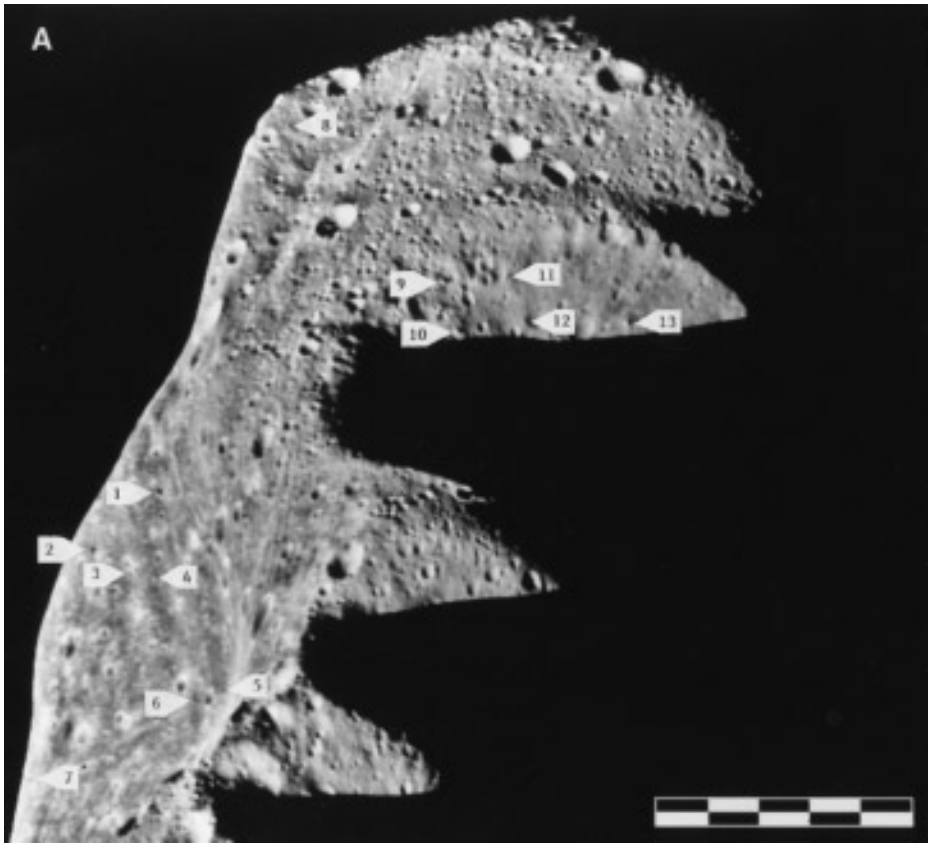
A
8
9
11
10
12
13
1
2
3
4
6
5
7

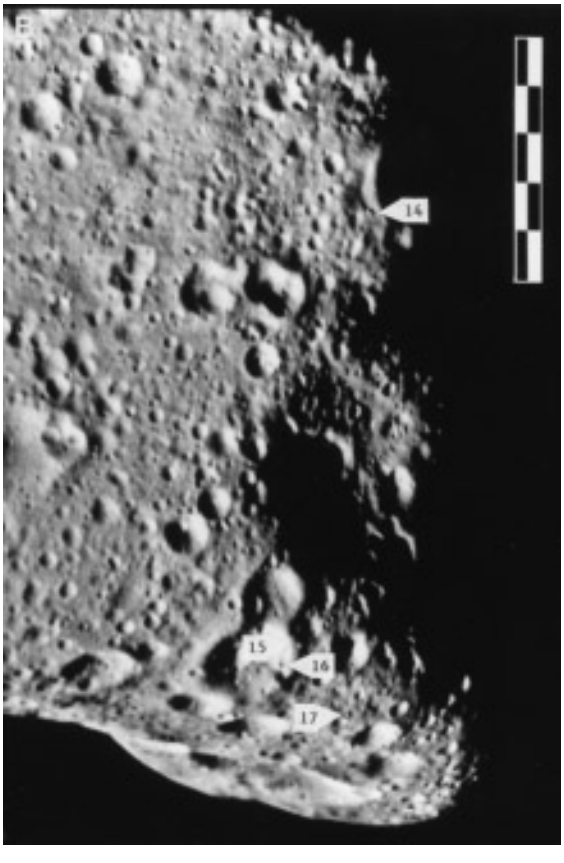
14
15
16
17

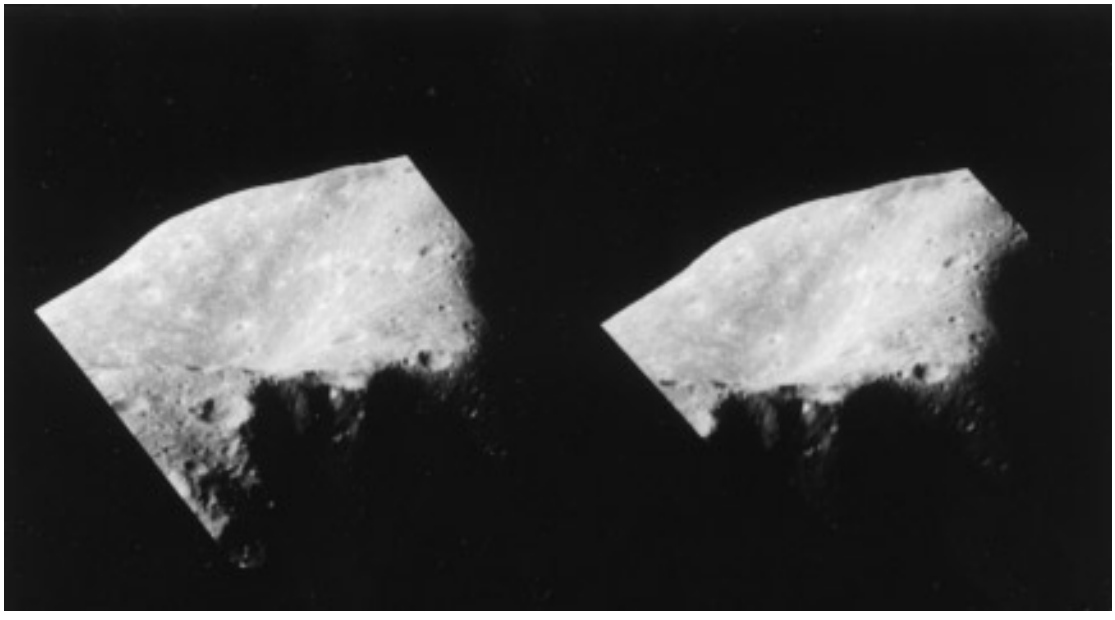

FIG. 3. Stereo pair using images 202562439 and 202562339 showing 7 blocks in crater Lascaux. Stereo viewing allows identification of blocks as small as 45 m across. The largest block in this figure (Block 1) is 130 m wide.

In addition to the 17 blocks identified relatively confidently, several dozen discrete PRFs (including PRF candidates) which might also be blocks are visible in the high-resolution mosaic of Ida. The features, however, are either too small, have too low a height-to-width aspect ratio, or do not stand out well enough against their background to be identified conclusively. Isolated PRFs might include partially buried blocks, weathered blocks with subdued outlines, piles of regolithic scree, protruding bedrock, raised crater rims, intersecting crater walls, and in a few cases perhaps imaging artifacts at the single pixel scale. Most of these PRFs are found on or near the rims of craters,

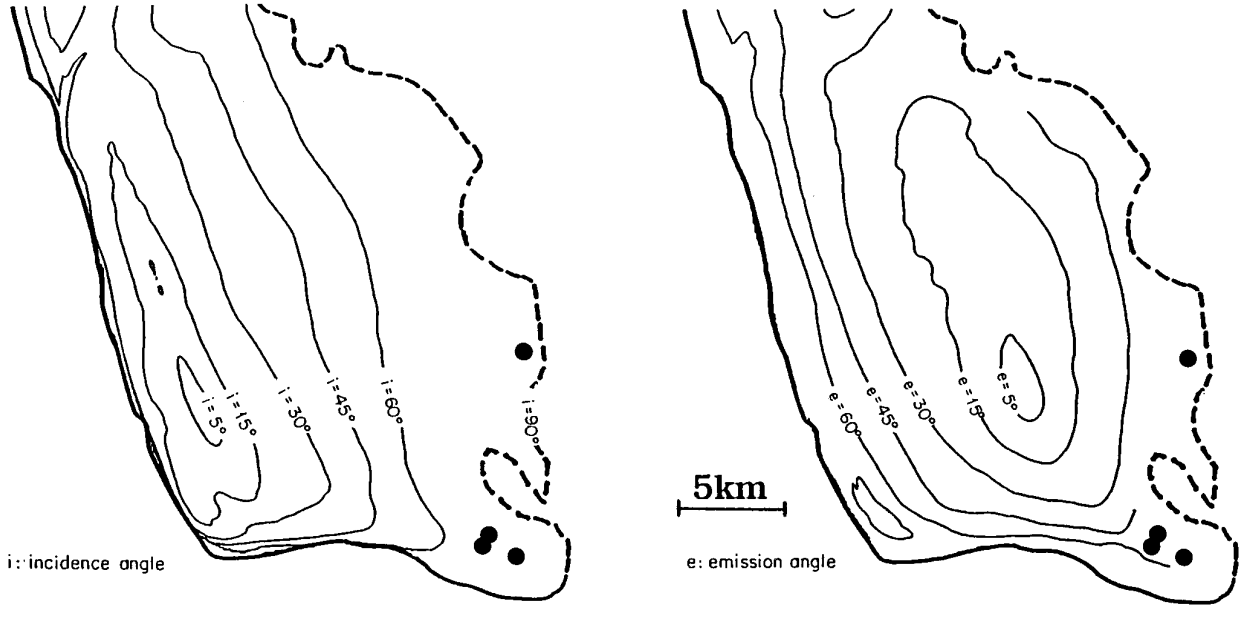

FIG. 4. Isophotes over the central and western regions (Regio Palisa), showing that few large blocks are seen there in spite of favorable photometric viewing. Bold black dots indicate block locations.

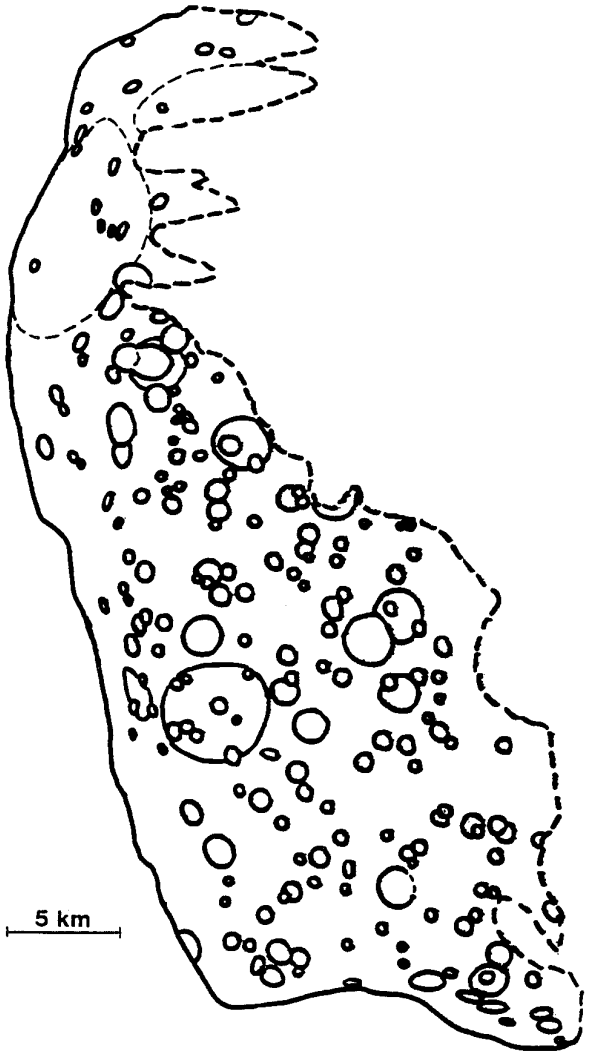

FIG. 5. Map of craters on Ida larger than 500 m in diameter and smaller than 10 km. The interiors of craters Lascaux and Mammoth, where most blocks are observed, are relatively sparsely cratered. This could be evidence for enhanced infilling and regolithic activity.

however, where ejecta blocks usually occur. Although few are found in regions where viewing is poor (e.g., along the limb), they are seen almost everywhere where photometric conditions are favorable. To first order, their distribution could be uniform (P. Lee *et al.* 1994).

2.2. Block Sizes

A cumulative plot of the size distribution of the 17 blocks identified on Ida is shown in Fig. 6. Size is estimated by evaluating the added width of pixels defining each block's illuminated face and by applying a corrective factor of up to $\sqrt{2}$ for blocks lying diagonally across pixel lines and samples. Five blocks are less than 60 m across; they can nevertheless be confidently identified because stereo coverage is available. Seven blocks are larger than 100 m. The largest blocks are ~150 m across. Uncertainties in the derived sizes are on the order of the pixel scale.

The remainder of our discussion focuses on the largest blocks. These are important because they can be inventoried with least uncertainty, and most standard (empirical) ejecta scaling laws offer predictions of maximum block sizes. We treat the blocks found on Ida as impact ejecta fragments, an assumption which will be justified in Section 2.4.1. No distinction will be made here between blocks located inside and outside (on the rim) craters. Although previous studies of ejecta block sizes have sometimes focused on blocks located on crater rims specifically (e.g., Moore 1971), not all have made this distinction (e.g., Gault *et al.* 1963). Moreover, at Meteor Crater for instance, large (≥20 m) blocks initially emplaced on the crater rim have slid or rolled downhill, coming to rest inside the crater bowl (Shoemaker and Kieffer 1974). Because block displacement subsequent to crater excavation (by crater wall slumping or impact induced spallation; see Section 2.4.4) is expected to occur readily in the low-gravity environment of an asteroid, making a formal distinction between blocks

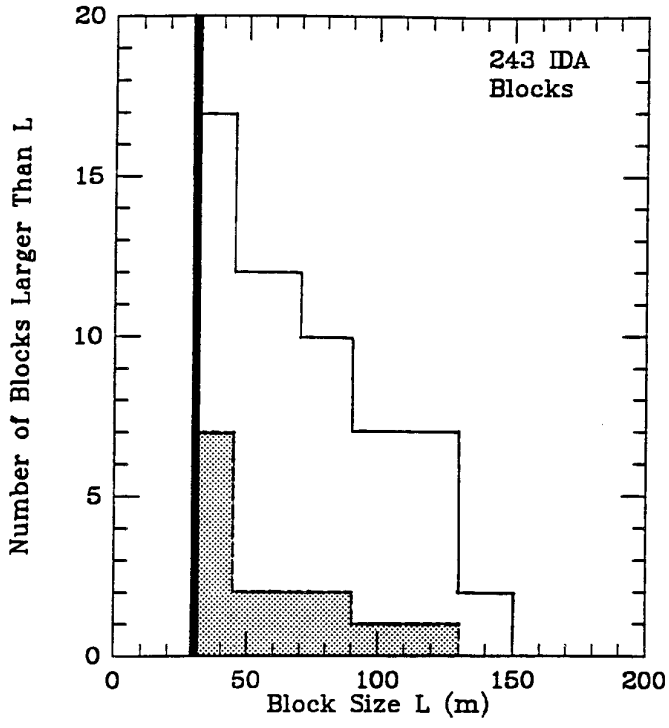

FIG. 6. Cumulative histograms of block sizes on Ida. The unshaded histogram takes into account all 17 blocks. The shaded histogram refers to the 7 blocks that lie within crater Lascaux (Blocks 1 to 7). The size distribution in the first case is less steep, illustrating how relatively few small blocks are identified outside of Lascaux. The availability of stereo coverage over Lascaux and not (or hardly) elsewhere contributes to the difference in histogram shape. The bold vertical line at 31 m marks the limit of resolution available in the mosaic (Fig. 1A).

located within and beyond 1 crater radius would be of illusory use.

From measurements on nuclear explosion craters and terrestrial impact structures, Gault *et al.* (1963) established that

$$m_L \sim 0.8\, M_e^{0.8}, \quad (1)$$

where M_e is the total mass ejected from a crater (in kg) and m_L is the mass of the largest fragment ejected (in kg). Equation (1) is approximate. Scatter in the data compiled by Gault *et al.* (1963) indicates that uncertainties of an order of magnitude are not unusual. Variables such as rock strength, joint spacing, and specific impact conditions can affect the final size of impact-generated blocks (Melosh 1989). Inhomogeneities in block age and hence in erosional state introduce additional variation. Also, in establishing Eq. (1), no distinction was made between blocks generated by the spall mechanism and those produced in the excavation flow. The largest crater considered by Gault *et al.* is the 22-km-wide Ries Basin in Germany which ejected blocks up to 1 km in size. These megablocks, some of which were apparently transported up to 6 km beyond the crater rim (Chao *et al.* 1978), are believed to have been mobilized by spallation, either as early, high-velocity but weakly-shocked spall (e.g., Melosh 1989) or as relict of low-velocity spallation with subsequent transport during emplacement (P. Schultz, personal communication). For Meteor Crater, on the other hand, another crater included in the Gault *et al.* study, the largest blocks considered (20–30 m across) were emplaced on the crater's rim late in the excavation phase (Shoemaker and Kieffer 1974). Equation (1) also does not distinguish between cratering regimes (gravity vs strength-dominated). We discuss this point in more detail below.

The volume, V, of material ejected from craters can be estimated from their apparent dimensions. Photoclinometry applied to fresh-looking craters on Ida yields $h \sim 0.15\, D$, where h is a crater's apparent depth and D its apparent diameter (Sullivan *et al.* 1996). Considering craters as spherical segments of depth h and of diameter D, their volume is then given by

$$V \sim 0.06\, D^3. \quad (2)$$

This expression is intermediate between that derived by McGetchin *et al.* (1973) for terrestrial and lunar craters in the hundreds of meters to kilometers radius range ($V = 2\pi TR^2$, where R is crater radius and $T \sim 0.04\, R$, the ejecta thickness at the crater rim; i.e., $V \sim 0.03\, D^3$), and that used by Veverka and Thomas (1979) based on observed crater depth-to-diameter ratios on the Moon and on Phobos ($h \sim 0.2\, D$; $V \sim 0.08\, D^3$). Although strictly an estimate of the volume of the *apparent crater* (displaced crater mass) which, for fresh craters, is generally greater by a factor of ~2 than the volume of the *excavation cavity* (the volume of material actually excavated and ejected from the crater) (e.g., Schultz *et al.* 1981), Eq. (2) is adequate here for achieving first order estimates of the total volume of ejecta produced on Ida, especially considering the significant infilling likely experienced by the older, large craters. Equation (2) should apply even to craters whose diameter approaches the mean radius of the target asteroid. Large craters on a curved surface have shallower profiles (smaller apparent depth-to-diameter ratios) than their bowl-shaped, terrestrial or lunar counterparts (e.g., Fujiwara *et al.* 1993), but we assume that the convexity of the preimpact target surface on asteroids roughly makes up for the shallower profiles of their larger craters.

Using Eq. (2), Eq. (1) can be rewritten as

$$L \sim 0.36\, D^{0.8}, \quad (3)$$

where D is crater diameter (in m) and L is the cubic size of the largest fragment ejected (in m). A dependence on material density is folded into Eq. (3) in the constant factor. We chose $\rho_{block} \sim 3.1\ g \cdot cm^{-3}$ and $\rho_{reg} \sim 2.1\ g \cdot cm^{-3}$ for the density of individual blocks and that of the excavated regolith, respectively[1]. According to Eq. (3), given a maximum crater diameter on Ida of ~11 km (Belton *et al.* 1994, Chapman *et al.* 1994a), the largest ejecta block is predicted to reach ~600 m in size. This is larger than the largest block actually identified, but by a factor ~4 only.

Moore (1971) studied the size distribution of blocks on the rims of lunar craters ranging from a few meters to ~100 km in diameter and found a relationship between maximum block size and crater diameter for blocks >1 m across. The relation yields maximum block sizes smaller than those predicted by Eq. (3),

$$L \sim (0.1 \text{ to } 0.3)\, D^{0.67}, \quad (4)$$

[1] From an analysis of Dactyl's orbital motion, Belton *et al.* (1995) estimate a bulk density for Ida of $2.6 \pm 0.5\ g \cdot cm^{-3}$ and favor a stony bulk composition consistent with chondrites. Anhydrous chondrites typically have densities of $3.5\ g \cdot cm^{-3}$ (Wasson 1985), while porosities are close to 0.11 and almost always ≤0.2 (Fujii *et al.* 1981, Hamano and Yomogida 1982). But just as lunar meteorites are distinctly stronger, less porous (by a factor of 2 or so), and denser than typical Apollo lunar consolidated regolith breccias, chondritic regolith breccias might not be representative of typical asteroidal regolithic material (McKay *et al.* 1989). By analogy, assuming that the porosity of coherent blocks on Ida is twice that of chondritic specimens, we attribute densities of $\sim 3.1\ g \cdot cm^{-3}$ to the blocks. The density of the regolith excavated by impacts, on the other hand, is likely less than that of the asteroid as a whole. If Ida is composed of rocky material of density similar to that of its blocks ($\sim 3.1\ g \cdot cm^{-3}$), the asteroid's bulk porosity would be ~0.16. Taking the upper regolith's porosity to be twice this value (~0.32), we derive a density for the surficial regolith of $2.1\ g \cdot cm^{-3}$.

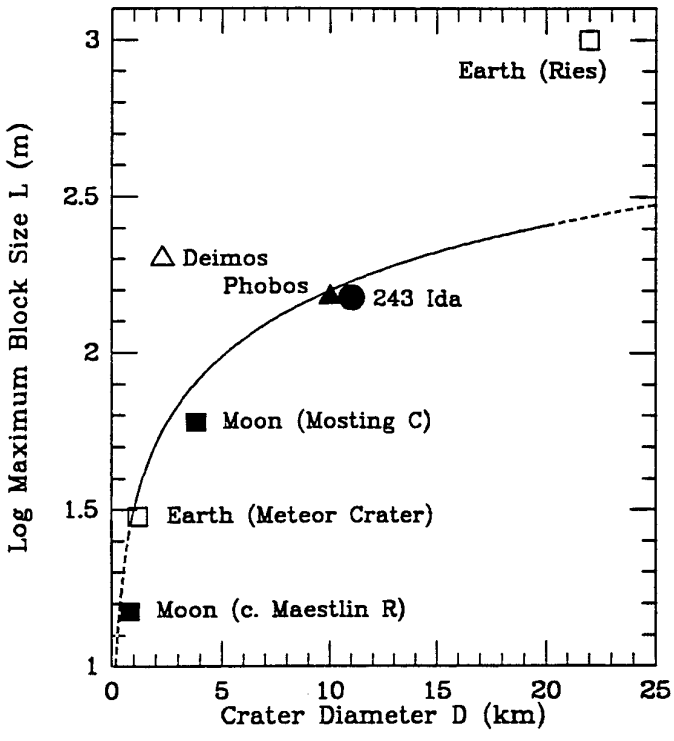

FIG. 7. Plot illustrating the evolution of maximum ejecta block size vs crater diameter, with examples from the Earth, the Moon, Phobos, Deimos, and Ida. The curve is Eq. (5) (see text), not a fit to the few points shown. Data for the 3.8-km diameter crater Mösting C and a 0.8-km crater near Maestlin R on the Moon are from Kosofsky and El-Baz (1970) and Schultz (1976, Plate 54c), respectively. Given that order of magnitude departures are possible, the size of the largest block found on Ida is in good agreement with empirical ejecta scaling laws established for rocky target bodies.

where L and D are in meters. Observed lunar block sizes often depart from this relation by a factor of ~2, likely for the same reasons as those listed earlier. Equation (4) would predict maximum block sizes on Ida of ~50–150 m, close to the observed maxima.

S. Lee *et al.* (1986) also examined block sizes in relation to crater sizes on Phobos, Deimos, and on the Moon. Blocks in the 30 to 150 m maximum size range on these bodies are found close to craters 1 to 10 km in diameter, as on Ida.

Thus, we find that the size relationship between Ida's largest blocks and its largest impact craters is, to first order, consistent with ejecta scaling relationships derived for the Earth, the Moon, Phobos, and Deimos (Fig. 7). Considering the uncertainties involved, the agreement is remarkable and suggests commonalities in the impact cratering process on the different objects and/or in the mechanical properties of their target materials. Maximum block sizes on Ida are consistent with the asteroid being a coherent rocky object exhibiting brittle fracture, although admittedly, little is known of what would characterize blockfields on, for instance, a more ductile asteroidal target.

From Eqs. (3) and (4), a general relationship between maximum ejecta block size, L, and crater diameter, D, can be derived for craters formed in rocky targets (10^3 m $\leq D \leq 2 \times 10^4$ m),

$$L \sim 0.25\ D^{0.7}, \tag{5}$$

with L and D in meters. Equation (5) would predict that the largest blocks on Ida are of order 170 m across, in reasonably good agreement with observation.

Implicit in the above comparison between craters of similar diameters on bodies with different surface gravities is that it is the target's mechanical response, more so than the specific cratering regime, that determines the relation between maximum ejecta block size and the energy of an impact (expressed in Eqs. (3)–(5) indirectly as the diameter of the resulting crater). The terrestrial craters used in deriving Eq. (1) span a range in diameters between a few meters and ~22 km and include both craters excavated under a gravity-dominated regime and craters formed under a strength-dominated one. It might thus appear desirable in Eq. (5) to distinguish between the two regimes. Moreover, many of the larger craters on the terrestrial planets were formed in a gravity-dominated regime, and craters of identical sizes on the Earth, the Moon, and on asteroid-sized bodies might have involved different formational energies. Under gravity scaling and for a given expended energy, the product $D \cdot g^{-1/4}$, where D is crater diameter and g the local gravitational acceleration, is to first order constant. On the Earth, where g is ~700 times greater than on Ida (~9.81 m $\cdot$ sec^{-2} vs ~$1.4 \cdot 10^{-2}$ m $\cdot$ sec^{-2}) craters are ~5 times smaller than their asteroidal equal-energy counterparts. Thus an 11 km, gravity-scaled crater on Ida would be equivalent to a 2 km terrestrial crater. Such crater scaling effects, however, are secondary compared to the other factors (e.g., target strength) that determine ejecta block size. That is, even if the correspondence between expended energy and crater diameter depends on the cratering regime and is therefore non-unique, the uncertainties in this correspondence are smaller than those introduced by variations in the target's mechanical properties. Surface gravity differences of 3 orders of magnitude translate into diameter differences of only a factor of 5 or so, and when introduced into Eq. (5), yield block cubic size differences of a factor of ~4 only. Comminution, on the other hand, depends mostly on the mechanical response of the target material to the delivery of impact energy, i.e., to local shock stresses and shock gradients. In particular, the size of the largest ejecta fragments found on the rim of fresh craters will reflect the last stages of crater formation where the flow field crosses isobars of material-dependent peak pressures (e.g., Schultz and Mendell 1978, Schultz *et al.* 1981). Factors

such as material strength and preimpact joint spacing, more so than the cratering regime per se or the crater size scale, will be critical to determining the ultimate size of the largest blocks (Gault and Heitowit 1963, Melosh 1989). For our purpose, Eq. (5) may thus be considered non-regime-specific.

2.3. Block Volumes

We next estimate the volume of ejecta represented by the blocks and the total volume of ejecta produced by craters on Ida. From the latter, estimates of upper limits for regional or "global" regolith thicknesses may be derived. Ratios of block volume to crater volume, on the other hand, allow hypotheses on the origin of the blocks to be tested.

Crater counts on the high-resolution mosaic of Ida yield ~200 craters with diameters ≥0.5 km, including craters Lascaux and Mammoth. (Figs. 1A and 5). Given that the fraction of Ida seen in the mosaic represents only ~30% of the asteroid's total area (Belton *et al.* 1994), the total number of craters larger than 0.5 km on Ida, assuming a uniform crater density, extrapolates to ~670. These would provide for ~6 craters in the 10^1 km diameter class, in agreement with the actual count of large craters from global imaging coverage of Ida (the 6 large craters are Lascaux Mammoth, Undara, Orgnac, Castellana, and Azzurra). With ejecta volume calculated via Eq. (2), the total volume of material excavated from all craters larger than 0.5 km in diameter represents ~500 km^3 or ~3% of Ida's present total volume ($V_{\mathrm{Ida}} \sim 16{,}100$ km^3). This estimate does not include the contribution from craters smaller than 0.5 km, but it nevertheless accounts for most of the ejecta produced because of the steepness of the power dependence of ejecta volume on crater size. Craters Lascaux and Mammoth alone contributed ~130 km^3 of ejecta, about 25% of all excavated material.

If all ejecta calculated were retained and distributed uniformly over the ~3800 km^2 of Ida's surface, a regolith layer on average ~130-m thick would result. This represents an upper limit: some ejecta must have been lost because of Ida's low escape velocity. The estimate may nevertheless be usefully compared with both model predictions for medium-sized asteroids and observations on Phobos: a ~100-m-deep regolith layer is predicted on asteroids ~100 km across (Housen *et al.* 1979), while a regolith depth of ~100–200 m was inferred for Phobos from examining the morphology of its grooves and craters (Thomas *et al.* 1979, Veverka and Thomas 1979).

If the total volume of ejecta was not distributed uniformly over Ida but accumulated preferentially in localized areas, large regional differences in regolith thickness could arise. Most of the ejecta generated at Stickney and retained on Phobos was deposited in the hemisphere centered on the large impact structure (Thomas 1979, Asphaug and Melosh 1993). By analogy, regional regolith thicknesses of order several hundred meters could be achieved in the hemispheres centered on Ida's largest craters, in which case burial or sinkage of even freshly formed blocks up to ~600 m across (the maximum block size predicted by Eq. (3)) is conceivable. In our earlier attempt to map and interpret the spatial distribution of the blocks as members of a single depositional unit, such variations in regolith depth could contribute significant bias by concealing specific subsets of the block population. Still more blocks could thus be present in Lascaux and Mammoth, only buried in the relatively deep regolith within these craters (see Section 2.4.5). Examination of the Ida mosaic reveals otherwise no clear indication of a thicker regolith cover around the two large impact structures (Fig. 1A).

The volume of material represented by the 17 blocks readily identified on Ida amounts to ~0.02 km^3. The 7 blocks that lie within or near the rim of Lascaux account for ~0.003 km^3 (Fig. 2A). This value is less than the volume of the largest block predicted via Eq. (5) alone ($v \sim 170^3$ m^3 ~ 0.005 km^3), suggesting that having all 7 blocks originating as ejecta fragments from that sole crater (or from any other one of Ida's 10-km class craters) would pose no difficulty volumewise.

2.4. Block Origin and Mode of Emplacement

2.4.1. Local derivation vs exogenous accretion. Blockfields on small, atmosphereless bodies are almost exclusively the result of impact processes (Garvin 1985). Accordingly, blocks on Ida are probably ejecta fragments produced and/or exposed following impact events. They are likely dominantly composed of materials derived from the target asteroid.

A possible alternative for the origin of the blocks is that they are accretionary fragments (impactors or fragments thereof accreted onto the asteroid without undergoing complete disruption), in which case the blocks would be composed of materials derived from impactors. Although this second possibility is unlikely in view of the present high collisional velocities between main belt asteroids (most collisions result in impactor disruption), the key arguments that allow this second possibility to be disregarded are worth examining quantitatively.

Bottke *et al.* (1994a) derive a mean collisional velocity $\langle V \rangle$ at Ida of ~3.55 km · sec^{-1}, along with most probable collisional velocities ranging from ~2.35 to 3.30 km · sec^{-1}. While such impact velocities would place crater formation in the low-velocity (<4.5 km · sec^{-1}) regime (a compressive one if a compactable particulate target surface were involved (Clark and McCarty 1963, Hartmann 1978), they are nevertheless high enough to result in the complete disruption of all but the strongest impactors (Melosh 1989).

A first order calculation on the survival of accreting blocks colliding into a hard, cohesive target surface indicates that the landing of blocks of density $\sim 3.1\ g \cdot cm^{-3}$ (see footnote 1) and of unconfined compressive static strength $\sim 10^8$ Pa, typical of that of basalts (Gault and Heitowit 1963, Blyth and de Freitas 1984), would preserve block integrity if impact velocities are $\leq 0.35\ km \cdot sec^{-1}$. Bottke *et al.* (1994a) among others show that such low impact velocities are rare today in the main belt: at the <1% level for Ida. That all blocks could actually result from the fragmentation of only one or two larger impactors allows for somewhat higher impact velocities, higher still if a soft, regolith-laden target is considered. Impactor survival, integrally or in resolvable fragments, might then be ensured for collision velocities up to $\sim 1\ km \cdot sec^{-1}$, depending in particular on the projectile's preimpact structure and on the ratio of projectile size to target regolith thickness. While collisions at such velocities are ~3 times more frequent (~3% level for Ida), the same general conclusion holds: impactor survival with any fragment resolvable in Galileo images is improbable at present.

The petrologic record in meteorite regolithic breccias, in particular in some polymict breccias which contain macroscopic clasts belonging to different meteorite classes, does attest that impactor material may on occasion survive intact in interasteroid collisions (Bunch *et al.* 1979, Bunch and Rajan 1988, Stöffler *et al.* 1988, McKay *et al.* 1989). But the meteorite regolithic breccias are ancient ($>3 \times 10^9$ years old) and result from collisional regimes and regolithic processes that might no longer prevail in the main belt today. Moreover, the fraction of allogenous meteoroidal material in the breccias is always very small, of order a few percent by weight only, and provides evidence for the survival only of relatively finely comminuted material.

Thus, while the principle of impactor survival on Ida may not be discounted altogether, it is improbable, especially for large fragments. The blocks found on the asteroid are most likely coarse ejecta fragments derived from the target. The fragments would include those blocks resulting directly from the comminution by impacts of coherent target material, preexisting blocks churned up in the regolith, and impact breccias (Arrhenius and Alfvén 1971, Cintala *et al.* 1982, McKay *et al.* 1989).

The presence of Dactyl, a satellite around Ida, raises an additional possibility. Like Ida, Dactyl is believed to have originated in the disruption of the Koronis parent body (KPB) some 10^9 years ago (e.g., Belton *et al.* 1994, Chapman *et al.* 1994b, Veverka *et al.* 1994, 1996). Those fragments that were imparted low relative velocities in the KPB disruption might have remained gravitationally bound, some accreting onto Ida as coherent blocks. Such material would have become part of Ida's regolith $\sim 10^9$ years ago, undergoing much of the processing experienced by its materials since. We argue in Section 2.4.5 that rocky blocks $\sim 10^2$ m across could survive $\sim 10^9$ years on an asteroid if shielded effectively in its regolith or if initially part of larger fragments. Some blocks on Ida could thus be individual surviving fragments from the KPB.

2.4.2. Comparison with Phobos and Deimos. Twelve of the 17 blocks on Ida lie within or near the rims of craters Lascaux and Mammoth (Figs. 1 and 2A). The association of such a significant fraction of observed blocks with the asteroid's largest craters points to a possible genetic relationship between the blocks and those craters. On Phobos, nearly all blocks are located close to large impact craters, and most large blocks are associated with Stickney (Thomas 1979). It is estimated that over 90% of the mass of all blocks on Phobos are actually located inside Stickney, suggesting that they were derived from the formation of that particular impact structure. In support of this interpretation, hydrocode modeling of the formation of Stickney indicates that its excavation involved extremely low flow velocities, as is the case for crater excavation on a low-gravity object under a nevertheless gravity-dominated regime[2] (Asphaug and Melosh 1993). Ejection velocities were apparently low enough to have allowed a substantial fraction of the ejecta to be retained, in particular in the immediate vicinity of the impact structure. On the basis of their basalt model and an impact velocity of $6\ km \cdot sec^{-1}$, Asphaug and Melosh estimated that excavation flow velocities of order only $3\ m \cdot sec^{-1}$ were evolved at Stickney and that ~80% of the ejecta mobilized in the flow was retained on Phobos. In this scenario, the large coherent blocks resting within Stickney and on the crater's rim were probably derived in the ''least-shocking'' and lowest-velocity tail portion of the crater-forming excavation flow.

On Deimos, the matching of blocks with their source crater is more difficult than on Phobos (Thomas 1979). S. Lee *et al.* (1986) argued on the basis of proximity and radial symmetry of their distribution that the largest blocks might have derived from Voltaire, the outer martian satellite's largest integral impact crater ($D \sim 2.3$ km).

Phobos and Deimos provide a basis of comparison for understanding cratering mechanics and ejecta dynamics on small bodies. Although the martian satellites are set in a gravitational environment that differs markedly from that of free-flying asteroids, the distribution of large ejecta blocks on Phobos appears to have been little influenced by the moon's proximity to Mars. With the specific example of Stickney at hand, a ready explanation for the origin of

[2] Because of their weak surface gravity, it might be tempting to assume that strength scaling prevails on all asteroid-sized bodies, at least for their smaller craters. Gravity-controlled cratering, however, may also be considered for craters of *any* size produced on asteorids (e.g., Melosh *et al.* 1992, Nolan *et al.* 1992, Asphaug and Melosh 1993, Asphaug *et al.* 1995). Craters of diameter D would form outside the strength regime either because they form in preexisting regolith ($D <$ 10–100 m) or because their impact energy fragments and weakens the region of crater formation before the evolution of the crater bowl ($D >$ 10–100 m).

the blocks found inside or near the rims of craters Lascaux and Mammoth on Ida is that they were derived directly from the formation of those craters. In the following sections, we use this straightfoward interpretation as our working hypothesis.

2.4.3. Spallation vs excavation. Laboratory experiments and field observations on the Earth and on the Moon indicate that large, coherent, and weakly shocked fragments produced during impact events are mobilized under two different ejection regimes (Melosh 1989). Blocks are generated either by spallation, the ejection of material resulting from the incidence, at a target's free surface, of shock waves capable of inducing tensile failure in surficial bedrock and/or lofting of preexisting loose surface fragments (Cintala *et al.* 1979; Hörz and Schaal 1981; Melosh 1984, 1985; Gratz *et al.* 1993), or by the crater excavation flow, the turbulent and highly sheared flow responsible for the excavation of the crater proper, which develops by rarefaction beneath the preimpact target surface from the residual velocity left in the wake of the shock wave. Specifically, coherent ejecta blocks are produced in the tail portion of this flow, where ejection velocities are lowest, and shock and shear levels may be relatively weak (excavation flow field crossing low peak shock isobars near the free surface) (e.g., Schultz *et al.* 1981). While both mechanisms operate for any given hypervelocity impact into a coherent target, the yields of each, in terms of their contribution to the production of large blocks, depend on the relative sizes of the target and projectile, and on the collision velocity. Hörz and Schaal (1981) argued that for an impact velocity of $\sim$5 km $\cdot$ sec^{-1}, a target (R_T) to projectile (R_P) radius ratio of $R_T/R_P \sim 100$ delineates the boundary between an ''infinite half-space'' and a ''finite''-sized target. For $R_T/R_P \gg 100$ (the infinite half-space case), the collisional energy is expended almost entirely in a pure cratering regime and the solid ejecta produced derives mostly from the excavation flow. For $R_T/R_P \ll 100$ (the finite-sized target case), a substantial fraction of the impact energy displaces target material by spallation, and the solid ejecta evolved may be dominated by spalls. In the intermediate case ($R_T/R_P \sim 100$), both the excavation flow and spallation mechanisms would contribute significant ejecta. Large ejecta blocks derived by excavation flow, however, tend to remain within or close to their source crater whereas spallation products do not.

We use Hörz and Schaal's (1981) criterion to discuss qualitatively differences in the relative importance of coarse spallation and excavation products. To determine which regime might have applied to the formation of craters Lascaux and Mammoth on Ida, we first estimate the size of the projectiles required to form those structures. From the gravity scaling equations of Schmidt and Housen (1987), for an impact at normal incidence angle into initially competent rock and for impactor and target of the same density, we have

$$R_P \sim 0.41\, D^{1.28}\, g^{0.28}\, v_i^{-0.56}, \tag{6}$$

where R_P is projectile radius (in m), D is crater diameter (in m), g is gravitational acceleration (in m $\cdot$ sec^{-2}) and v_i is impact velocity (in m $\cdot$ sec^{-1}). For $D \sim 11$ km and $g \sim 1.4 \times 10^{-2}$ m $\cdot$ sec^{-2} (Belton *et al.* 1994), an impact velocity of 3 km $\cdot$ sec^{-1} would call for projectiles $\sim$200 m in radius. This yields a target to projectile radius ratio of $R_T/R_P \sim 86$, close to 100. Lascaux and Mammoth could thus have formed in the intermediate regime, spawning coarse ejecta fragments via both the excavation flow and spallation mechanisms. As most blocks on Ida appear to be restricted to the interior and rim of its largest craters, if the blocks were derived directly from those structures (our working hypothesis), excavation flow (specifically its low-velocity, weakly shocking tail portion) more likely than spallation was their prime mode of emplacement. If, on the other hand, the blocks did not originate in Lascaux and Mammoth, they could include a significant fraction of spallation fragments, and another emplacement (and clustering) mechanism would have to be sought (see Section 2.4.4).

The above discussion provides only a qualitative decription of the possible outcomes of impacts of various magnitudes on Ida. As used here, the Hörz and Schaal (1981) criterion is largely arbitrary: the actual transition value of the R_T/R_P ratio will depend on the composition, structure, strength, shape, impact location, impact angle, and relative velocity of the target and projectile, and may be significantly different from 100.

2.4.4. Alternative hypotheses. Alternative explanations for the spatial distribution of Ida's blocks have been proposed.

Geissler *et al.* (1994, 1995) note that the portions of the eastern and western regions where most blocks are found coincide with the asteroid's leading sides in a rotational sense. The implication is that the spatial association of most blocks with Ida's largest craters might have no direct genetic underpinning. Geissler *et al.* show that the block distribution is consistent with a dynamical model in which the blocks are ejecta fragments launched into partial or temporary orbits about Ida and are subsequently swept up upon fallback by the asteroid's rotational leading surfaces. As pointed out by its authors, while plausible, this scenario is difficult to test conclusively, partly because the rotational trailing side in the eastern region is not visible at adequate resolution in the Galileo images to allow ascertaining a dearth of blocks there. Geissler *et al.*'s (1995, 1996) model also suggests that a distinct rotational asymmetry in block distribution develops only for the fraction of retained ejecta launched initially at relatively high (yet at subes-

cape) velocity; the asymmetry subsides for lower velocity ejecta. For any high-velocity large ejecta block evolved, however, a substantial number of large blocks launched at lower velocities is usually also produced (e.g., Vickery 1987, Nakamura and Fujiwara 1991). The clustering of the main blockfield on Phobos within and on the rim of Stickney (Thomas 1979) and hydrocode modeling of the formation of that crater (Asphaug and Melosh 1993) indeed suggest that most blocks retained on small bodies were launched at velocities far below escape. Had the sweep-up mechanism dominated the pattern of block fallback on Phobos, a more uniform distribution would have resulted there. Thus, while the sweep-up process may have played a significant role in the recovery and distribution of higher-velocity spalled ejecta or of the smaller-sized ejecta associated with the more dynamic portions of the excavation flow (finer ejecta from crater Azzurra could be responsible for defining the extensive color/albedo unit which dominates the northern and western hemispheres of Ida as suggested by Geissler *et al.* (1996)), it is less clear whether the same process was also the prime contributor to the clustered distribution of large blocks at Lascaux and Mammoth.

Another explanation for the block distribution considers the migration of ejecta fragments in Ida's weak gravity environment and their collection in local lows in dynamic height (to be distinguished on irregular-shaped spinning bodies from simple topographic lows (Thomas 1993)). Free blocks on small bodies may be seismically destabilized and roll or slide, or be lofted (spalled) by violent impacts, becoming trapped as they settle in craters and other depressions. First order measurements based on the shape model for Ida indicate that crater Lascaux corresponds to a distinct regional low in dynamic height. Crater Mammoth, on the other hand, appears to lie on a dynamic slope, perhaps an artifact resulting from our poorer knowledge of the shape of Ida in Mammoth's area; the large crater more likely is a local dynamic low as well (Fig. 8). The blocks clustered about these craters might have originated from a relatively distant source and were collected inside or near the craters following ballistic hops, rolling, or sliding. That some blocks have experienced this mode of emplacement is suggested by the observation that the 150-m-sized boulders in the western region are associated with craters much smaller than Lascaux or Mammoth: Padirac is only 2.2 km across. If Eq. (5) were to hold strictly and target lithology on Ida did not vary significantly from Pola Regio to Vienna Regio, blocks associated with Padirac would be no larger than ~55 m across. Block migration (including via the Geissler *et al.* process) followed by trapping in a dynamic low could offer a needed alternative in this case. But as we noted earlier, Eq. (5) is subject to large deviations, and lithology might well vary laterally on Ida (Sullivan *et al.* 1996). Ultimately, because several regional lows in dynamic height other than Lascaux occur in the hemisphere of Ida viewed at high resolution and no blocks are observed there (Fig. 8), dynamic lows likely played no more than a secondary role in arresting migrating blocks.

The presence of ''chutes'' in proximity to blocks in crater Mammoth (Fig. 2A) (Belton *et al.* 1994, Greeley *et al.* 1994, Sullivan *et al.* 1996) suggests that some post-excavation downhill sliding of regolith material has occurred. Some might have been triggered by or accompanied ejecta block migration. Aside from potentially high-velocity secondary impacts possible only under peculiar geometries given Ida's irregular shape, the maximum reimpact velocity of any ejecta fragment launched off of Ida is normally equal to the maximum escape velocity from the asteroid's surface ($\sim 20\ \mathrm{m \cdot sec^{-1}}$) plus the maximum instantaneous rotational velocity of the asteroid ($\sim 10\ \mathrm{m \cdot sec^{-1}}$). Thus, secondary impacts on Ida usually take place at velocities $\leq 30\ \mathrm{m \cdot sec^{-1}}$, producing at most moderate compression of the regolith. Slopes of particulate material near angle of repose could nevertheless be destabilized and lead to chutes. No boulder tracks have been reliably identified on Ida, but estimates of possible track depths indicate that they would be unresolved (Sullivan *et al.* 1996). The possibility that the blocks on Ida resulted from the fragmentation of a smaller number of larger boulders cannot be excluded either.

2.4.5. How old are the blocks? The cosmic ray exposure (CRE) age of most Apollo lunar rock samples reveal surface residence times $\geq 10^6$ years and $\ll 10^9$ years (Reedy *et al.* 1983, Heiken *et al.* 1991). Residence times $\geq 10^9$ years seldom occur on the Moon because exposed blocks are eventually removed by impact-related processes. Blocks may be directly disrupted in collisions or be buried in fresher ejecta deposits. Impact-induced spallation and other surface movement (sliding, tumbling) impose additional mechanical duress on the more poorly consolidated fragments (Arvidson *et al.* 1975). Micrometeortic sandblasting also abrades exposed lunar blocks at a rate of ~1 mm per 10^6 years (Ashworth 1977). On a 10^9 year timescale, this latter process alone would reduce meter-sized rocky fragments to a finely comminuted soil. Depending on the local evolution of the regolith, on local topographic slopes, and on material strength, blocks on the Moon actually experience complex histories of fragmentation, burial, and reexposure (e.g., Arvidson *et al.* 1975, Burnett *et al.*1975), leading to a range of survival times. As a result, crisp-looking boulders associated with morphologically degraded lunar craters are not uncommon. Also, Monte Carlo simulations by Hörz *et al.* (1975) of the collisional life expectancy of lunar rocks, although difficult to extrapolate reliably to large boulders because of scaling unknowns, suggest that the median survival time of blocks 10^2 m in

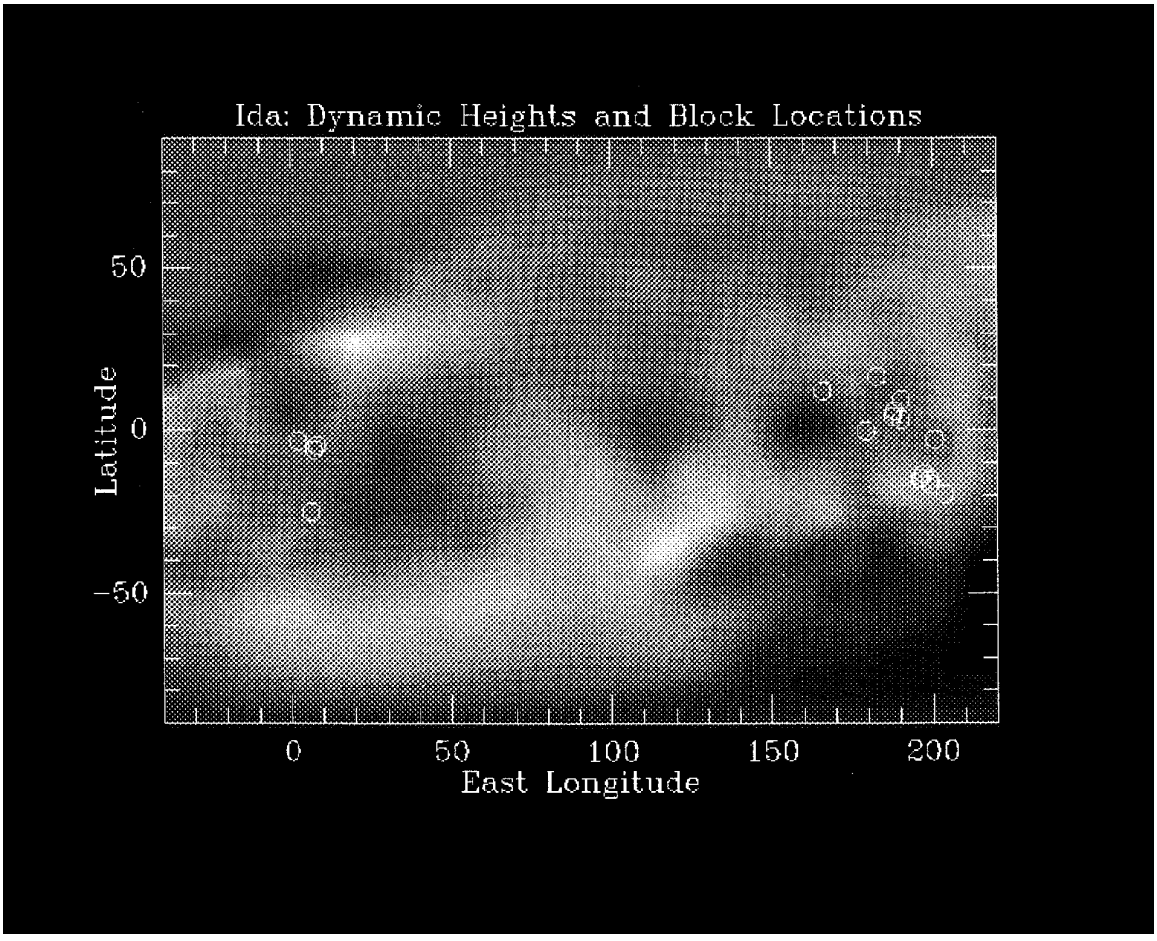

FIG. 8. Map of dynamic heights on Ida. Light areas correspond to highs, dark areas to lows. Block locations are indicated by white circles. The map shows that crater Lascaux (~10°N, 185°E) coincides with a regional low in dynamic height. Crater Mammoth (~15°S, 200°E), on the other hand, is shown to lie on a steep dynamic slope, but this may be an artifact resulting from poor constraint of Ida's shape model in this area. Several regional lows, although imaged at high resolution, are devoid of blocks (at least in blocks >120 m), suggesting that lateral migration and trapping in dynamic lows is likely not the prime cause for the observed block distribution.

size could reach 10^9 years or more under the present lunar impactor flux. Boulders on asteroids are expected to be subject to the same removal mechanisms as on the Moon, only on timescales that differ due to differences in surface gravity, impactor population, collisional velocity regimes, regolith production and turnover rates, and target strength.

A starting point to estimating the life expectancy of asteroidal boulders is to consider the exposure record preserved in meteorites. The CRE age of a meteorite dates the time of fragmentation of its parent meteoroid when it was reduced to a size of a few meters or less. Because small objects are more easily disrupted than larger ones, the CRE age of meteorites provides a lower limit on the life expectancy of asteroids $\geq 10^1$ meters across. CRE ages of iron meteorites commonly lie in the range 10^8–10^9 years (Bogard 1979). Because these ages are greater than possible timescales for asteroidal orbital evolution into and within the inner Solar System (10^6–10^8 years (e.g., Wetherill 1974, Farinella *et al.* 1994)), most of the CRE in iron meteorites likely was acquired while the objects resided in the main belt, within meter-sized meteoroids. From this, we infer that iron meteoroids 10^1–10^2 m in size can probably survive several 10^9 years or more in the present collisional environment of the main belt.[3] The CRE ages of nearly all stony meteorites, on the other hand, fall in the range 10^5–6×10^7 years, significantly less than that of iron meteorites (Bogard 1979). (The greater CRE ages of irons is usually attributed to their greater mechanical strength which enhances their ability to survive interasteroidal collisions.) Since the range in CRE ages of stony meteorites overlaps with that of possible dynamical lifetimes, these

[3] The life expectancy in the main belt is controlled by collisions among asteroids (a collisional lifetime is defined), whereas that in inner planet-crossing space is controlled by dynamical evolution until a planet or the sun is intercepted (dynamical lifetime).

meteorites could have acquired the bulk of their CRE either during their residence in the main belt or during their transfer from the main belt to the Earth. Regardless, the maximum recorded CRE ages in stony meteorites implies that meter-sized stony meteoroids survive probably no longer than a few 10^7 years in the main belt. Larger stony asteroids in the main belt would have somewhat greater life expectancies: by extrapolation, we estimate that 10^1–10^2-m-sized asteroids could survive several 10^7 to $\sim 10^8$ years.

Another approach to the problem is to consider the impactor flux in the main belt and to compare the corresponding delivered impact energy frequency distribution with the disruption threshold (or yield strength) of target objects. Typically, asteroids in the 10^1–10^2 m radius range are found to have lifetimes with respect to catastrophic disruption of a few 10^7 to 10^8 years (e.g., Dohnanyi 1969, Bottke *et al.* 1994b). With a first order calculation, Belton *et al.* (1994) found life expectancies of ~ 3 to 8.10^7 years for (stony) blocks 30 to 100 m across, in agreement with standard results.

The two preceding approaches to the block lifetime problem (CRE ages in meteorites and dynamical studies) thus yield consistent results. Both suggest that stony objects $\sim 10^2$ m in size have life expectancies in the main belt of order 10^8 years. The lifetimes derived, however, pertain strictly to free-flying boulders, that is to individual asteroids $\sim 10^2$ m across. Blocks resting on larger asteroids are effectively shielded from direct impactor hits over an entire half-space, a circumstance which alone doubles their lifetime against collisional disruption. In addition, episodes of burial in a protective regolith further reduce block exposure to impacts, extending their life expectancy by a factor approximately inversely proportional to the fraction of time the blocks are exposed. Successive episodes of exhumation and burial could have resulted from impact-induced jostling of the regolith and the deposition and departure of regolith covers (Cintala *et al.* 1979, Hörz and Schaal 1981). Because gravity is weaker on small bodies and seismic effects are enhanced, episodes of block burial and exposure could occur more repeatedly on asteroids than on the Moon. The exposure time fraction is difficult to estimate as it depends on the asteroid's size (mass), the applicable cratering regime, local regolith thicknesses and the competition over time between burial and excavation with respect to regolith depth (Housen *et al.* 1979). Interpolating between models of 10 and 300 km asteroids on which gravity scaling was set to apply (Housen *et al.* 1979), we find that 50 km asteroids like Ida might experience both excavation and burial to a depth of ~ 100 m over time intervals of similar duration, of order 10^8 years. Blocks $\sim 10^2$ m in size near the surface of Ida could thus be shielded from external hazards for about half their existence, for $\sim 10^8$ years at a time. This effectively doubles their life expectancy with respect to that of similar-sized blocks on a regolith-free asteroid. By combining the two preceding lifetime-doubling factors, a total four-fold increase in the survival time of $\sim 10^2$-m-sized boulders compared to similar-sized free-flying asteroids is achieved. The 10^2-m-sized (rocky) blocks in craters Lascaux and Mammoth could then easily be up to several 10^8 to 10^9 years old, an age that would rougly coincide with the probable age of the large impact structures according to some models (Belton *et al.* 1994, Chapman *et al.* 1994b, Sullivan *et al.* 1996).

Belton *et al.* (1994) noted that because craters 1–10 km in diameter are likely required to produce 100-m-sized ejecta blocks, one or more craters in this size range might have formed on Ida in a relatively recent past, i.e., during the past 3 to 8×10^7 years, their estimated lifetime against collisional disruption for 30–100 m blocks. Younger ages still were believed possible if there have been enhanced collisions with Koronis family asteroids (Belton *et al.* 1994). Geissler *et al.* (1996) suggest that since craters Lascaux and Mammoth have thoroughly degraded morphologies and are possibly as old as Ida itself ($\sim 10^9$ years old), the presence of blocks ≤ 3 to 8×10^7 years old in those structures would imply that the blocks originated elsewhere, possibly in crater Azzurra, a 10-km-diameter impact structure believed to be relatively fresh. The consideration of block shielding by a regolith-bearing asteroid, however, allows for significantly increased block survival times and could alleviate the need to have a 1–10 km crater form on Ida relatively recently. The anticorrelation noted in Section 2.1 between block surface density and crater density can be interpreted as being at least partly due to enhanced block preservation in localities of more dynamic regolith thickness and activity. Large crater bowls such as Lascaux and Mammoth serve as efficient traps for loose and migrating regolith material, and may be subject to mass-wasting on relatively large scale. The anticorrelation does not imply that blocks on Ida are found preferentially in craters that would be young. Rather, it illustrates how 10^2 m blocks might have benefitted from enhanced collisional shielding in the relatively dynamic regolith environment associated with large (and likely ancient) craters. In Palisa Regio, in contrast, large craters are absent and so are thick regolith blankets (Sullivan *et al.* 1996). Any large block landed in the region would be afforded less protection than in Lascaux or Mammoth, and block lifetimes could be reduced by a factor ~ 2. This, along with the fact that large block-producing craters are absent there, might help explain why large (≥ 120 m across) blocks appear rare in the central portion of Ida.

In support of the survivability of impact-generated rocks on asteroids, we add that meteorite regolithic breccias typically preserve ancient asteroidal regoliths 10^9 to $\sim 4.3 \times 10^9$ years old (e.g., McKay *et al.* 1989). Rather than requiring that these breccias derived from large, long-surviving

breccia meteoroids, the preservation of ancient asteroidal regoliths more likely indicates that the shielding of brecciated ejecta components on asteroids can be effective over several eons.

3. BLOCKS ON OTHER ASTEROIDS?

The relative success encountered with ejecta scaling laws derived for the Earth, the Moon, Phobos, and Deimos in predicting maximum block sizes on Ida prompts an application to Dactyl and Gaspra and speculation about block sizes on other asteroids.

Ida's satellite Dactyl is 1.4 km in diameter. The portion of its surface imaged at a resolution of 39 m/pixel bears integral craters up to ~300 meters across. Equation (5) predicts that on a relatively coherent rocky body, blocks no larger than ~15 m would be associated with such small craters. Blocks of this size would remain undetectable in the available Galileo images. Two large PRFs ~100 m across are seen on Dactyl (Veverka *et al.* 1996). The features are located within 300-m-diameter crater-like formations (crater Acmon and the "high albedo feature") but are poorly resolved. Considering the uncertainties associated with Eq. (5), the PRFs could be unusually large ejecta masses derived from craters on Dactyl. Alternatively, the features could be ejecta fragments accreted from Ida, i.e., products of secondary impacts (Veverka *et al.* 1996, Geissler *et al.* 1996).

No block is readily identifiable on Gaspra (Belton *et al.* 1992, Veverka *et al.* 1994). A few PRFs that are possible candidates may be seen, but all are too near the limit of resolution to allow confident identification. Equation (5) predicts that the size of the largest ejecta fragments expected on Gaspra, given the observed maximum crater diameter of ~3 km, is ~70 m. Moore's (1971) relation (Eq. (4)) predicts maximum block sizes of order 20–65 m. S. Lee *et al.* (1986) indicate that 3-km craters are accompanied by blocks usually no larger than ~70 m in size. Thus, the lack of readily identifiable blocks on Gaspra is not surprising. The largest blocks predicted by empirical scaling laws would be less than a factor of ~2 larger than the best available pixel resolution in Galileo images (54 m).

433 Eros, an S-type asteroid with approximate dimensions 13 × 15 × 36 km and a rotation period of 5.27 hr, is the target of the upcoming NEAR mission. Surface thermal inertia measurements suggest that its surface is probably not as dusty as the surface of the Moon and may have significant rocky exposures (Lebofsky and Rieke 1979). The size of the largest integral crater supported by Eros is unknown, but if the average ratio of largest crater diameter to mean body diameter for Gaspra and Ida (~0.3) applies, the ~20-km-diameter asteroid might bear craters 6 km across. Equation (5) then predicts that ejecta blocks up to ~100 m in size could be present. The imaging system on the NEAR spacecraft will achieve spatial resolutions of $9.5 \times 10^{-5} \times 1.6 \times 10^{-4}$ rad/pixel (rectangular pixels) (Cheng *et al.* 1994), i.e., 4 m/pixel during the final 2D orbit phase (R being Eros's mean radius). This will allow shape modeling and composition mapping of individual blocks. Geissler *et al.* (1995) have already modeled ejecta reaccretion and regolith redistribution on Eros, obtaining results qualitatively similar to those for Ida. NEAR observations of Eros will provide an interesting opportunity to further examine ejecta dynamics on small, fast-rotating bodies.

4 Vesta is the largest V-type asteroid known and is thought to be the original parent body of the HED or basaltic achondrite meterorites (e.g., Drake, 1979, Greenberg and Nolan 1989). The asteroid is 520 km in diameter, rotates in 5.34 hr, and on the basis of rotation-dependent spectral variations, may bear a ~140-km-wide impact basin, exposing olivine-rich and/or diogenite-like mantle materials (Gaffey 1983, 1995). Application of Eq. (5) to Vesta suggests ejecta megablocks up to ~1 km across could be associated with such a structure, somewhat smaller than the 4–10-km-sized V- and J-type asteroids believed to have been spalled off Vesta (Binzel and Xu 1993).

4. CONCLUSION

Seventeen blocks are identified in the high-resolution mosaic of 243 Ida. Most are located within or on the rims of craters Lascaux and Mammoth, the two largest impact structures visible in the mosaic. The spatial distribution, maximum sizes, and integrated volume of the blocks are consistent with the straightforward hypothesis that those at Lascaux and Mammoth derived directly (or after some fragmentation) from the formation of those impact structures. Conformity to empirical ejecta scaling laws suggests that cratering mechanics on Ida are to first order similar to those that apply on the Earth, the Moon, Phobos, and Deimos, all of which are rocky target bodies. The blocks on Ida may be composed of rocky target material and were likely mobilized by both excavation and spallation. Some could be surviving fragments accreted from the disruption of the Koronis parent body. The blocks clustered near Lascaux and Mammoth were probably mobilized as low-velocity, weakly shocked ejecta in the tail portion of the excavation flow that produced those craters. The interiors and rims of Lascaux and Mammoth are apparently less densely cratered than the central and western regions of Ida (Regio Palisa), possibly an indication of enhanced resurfacing within ancient, regolith-filled craters. Such activity, along with the shielding afforded by the asteroid's bulk, may have allowed ~10^2-m-sized blocks to survive significantly longer than free-flying asteroids of the same size, perhaps up to several 10^8 to ~10^9 years. There may thus be no contradiction in genetically associating rela-

tively crisp-looking blocks with ancient, degraded impact structures. Other modes of emplacement, such as the preferential sweep-up of launched blocks by the asteroid's rotational leading sides or the trapping of migrating blocks in areas of low dynamic height, may have contributed, albeit secondarily, to the observed block distribution. Our working hypothesis is most strongly supported by its consistency with the spatial distribution of ejecta blocks on the only other well-imaged small body in the solar system with a large crater, Phobos.

Blocks on Dactyl and on 951 Gaspra, if any, are expected to be too small to be identifiable in Galileo images. The dimensional characteristics of 433 Eros suggest that integral craters ~6 km across could be present, yielding maximum block sizes of order 100 m. Such blocks would be interesting targets for detailed examination during the upcoming NEAR mission. Similarly, km-sized megablocks might occur on 4 Vesta, adding to the long list of interesting objectives for the future exploration of this large asteroid.

ACKNOWLEDGMENTS

We are grateful to Steven Lee and Peter Schultz for helpful reviews. This work also benefitted from discussions with Mike Gaffey and Paul Geissler. Brian Carcich and Sarah Calvo at Cornell contributed to the compilation of the block data for Ida. This work was supported by NASA Grant NAGW 2186 and by the Galileo Project.

REFERENCES

Arrhenius, G., and H. Alfvén 1971. Asteroidal theories and experiments. In *Physical Studies of Minor Planets* (T. Gehrels, Ed.), pp. 213–223. NASA SP-267.

Arvidson, R., G. Crozaz, R. J. Drozd, C. M. Hohenberg, and C. J. Morgan 1975. Cosmic ray exposure ages of features and events at the Apollo landing sites. *Moon* **13,** 259–276.

Ashworth, D. G. 1977. Lunar and planetary impact erosion. In *Cosmic Dust* (J. A. M. McDonnell, Ed.), pp. 427–526. Wiley, New York.

Asphaug, E., and H. J. Melosh 1993. The Stickney impact of Phobos: A dynamical model. *Icarus* **101,** 144–164.

Asphaug, E., J. M. Moore, D. Morrison, W. Benz, M. C. Nolan and R. Sullivan 1996. Mechanical and geological effects of impact cratering on Ida. *Icarus* **120,** 158–184.

Belton, M. J. S., J Veverka, P. Thomas, P. Helfenstein, D. Simonelli, C. Chapman, M. E. Davies, R. Greeley, R. Greenberg, J. Head, S. Murchie, K. Klaasen, T. V. Johnson, A. McEwen, D. Morrison, G. Neukum, F. Fanale, C. Anger, M. Carr, and C. Pilcher 1992. Galileo encounter with 951 Gaspra: First pictures of an asteroid. *Science* **257,** 1647–1652.

Belton, M. J. S., C. R. Chapman, J. Veverka, K. P. Klaasen, A. Harch, R. Greeley, J. W. Head III, A. McEwen, D. Morrison, P. C. Thomas, M. E. Davies, M. H. Carr, G. Neukum, F. P. Fanale, D. Davis, C. Anger, P. J. Gierasch, A. P. Ingersoll, and C. B. Pilcher 1994. First images of asteroid 243 Ida. *Science* **265,** 1543–1547.

Belton, M. J. S., C. R. Chapman, P. C. Thomas, M. E. Davies, R. Greenberg, K. Klaasen, D. Byrnes, L. D'Amario, S. Synnott, T. V. Johnson, A. McEwen, W. J. Merline, D. R. Davis, J-M. Petit, A. Storrs, J. Veverka, and B. Zellner 1995. Bulk density of asteroid 243 Ida from the orbit of its satellite Dactyl. *Nature* **374,** 785–788.

Binzel, R. P., and S. Xu 1993. Chips off of asteroid 4 Vesta: Evidence for the parent body of basaltic achondrite meteorites. *Science* **260,** 186–191.

Blyth, F. G. H., and M. H. de Freitas 1984. *A Geology for Engineers,* 7th ed. English Language Book Society, Edward Arnold, London.

Bogard, D. D. 1979. Chronology of asteroid collisions as recorded in meteorites. In *Asteroids* (T. Gehrels, Ed.), pp. 558–578. Univ. of Arizona Press, Tucson.

Bottke, Jr., W. F., M. C. Nolan, R. Greenberg, and R. A. Kolvoord 1994a. Velocity distributions among colliding asteroids. *Icarus* **107,** 255–268.

Bottke, Jr., W. F., M. C. Nolan, R. Greenberg, and R. A. Kolvoord 1994b. Collisional lifetimes and impact statistics of near-Earth asteroids. In *Hazards Due to Comets and Asteroids* (T. Gehrels, Ed.), pp. 337–357. Univ. of Arizona Press, Tucson.

Bunch, T. E., S. Chang, U. Frick, J. Neil, and G. Moreland 1979. Carbonaceous chondrites—I. Characterization and significance of carbonaceous chondrite (CM) xenoliths in the Jodzie howardite. *Geochim. Cosmochim. Acta* **43,** 1727–1742.

Bunch, T. E., and R. S. Rajan 1988. Meteorite regolithic breccias. In *Meteorites and the Early Solar System* (J. F. Kerridge and M. S. Matthews, Eds.), pp. 144–164. Univ. of Arizona Press, Tucson.

Burnett, D. S., R. J. Drozd, C. J. Morgan, and F. A. Podosek (1975). Exposure histories of Bench Crater rocks. *Proc. Lunar Sci. Conf. 6th,* 2219–2240.

Chao, E. C. T., R. Hüttner, and H. Schmidt-Kaler 1978. *Principal Exposures of the Ries Meteorite Crater in Southern Germany. Description, Photographic Documentation and Interpretation.* Bayerisches Geologisches Landesamt, Prinzregentenstraße 28, D 8000 München 22.

Chapman, C. R., M. J. S. Belton, J. Veverka, G. Neukum, J. Head, R. Greeley, K. Klaasen, D. Morrison, and The Galileo Imaging Team 1994a. First Galileo image of asteroid 243 Ida. *Lunar Planet. Sci. Conf. XXV,* 237–238. [Abstract]

Chapman, C. R., W. J. Merline, D. R. Davis, J. Veverka, M. J. S. Belton, T. V. Johnson, and The Galileo Imaging Team 1994b. Ida's satellite: Its origin and impact history. *Bull. Am. Astron. Soc.* **26,** 1157. [Abstract]

Cheng, A. F., J. Veverka, C. Pilcher, and R. W. Farquhar 1994. Missions to near-Earth objects. In *Hazards Due to Comets and Asteroids* (T. Gehrels, Ed.), pp. 651–670. Univ. of Arizona Press, Tucson.

Cintala, M. J., J. W. Head, and J. Veverka 1978. Characteristics of the cratering process on small satellites and asteroids. *Proc. Lunar Planet. Sci. Conf. 9th,* 3803–3830.

Cintala, M., J. W. Head, and L. Wilson 1979. The nature and effects of impact cratering on small bodies. In *Asteroids* (T. Gehrels, Ed.), pp. 579–600. Univ. of Arizona Press, Tucson.

Cintala, M., J. B. Garvin, and S. J. Wetzel 1982. The distribution of blocks around a fresh lunar mare crater. *Lunar Planet. Sci. Conf. XIII,* 100–101. [Abstract]

Clark, L. V., and J. L. McCarty 1963. *The Effect of Vacuum on the Penetration Characteristics of projectiles into Fine Particles.* NASA TND-1519.

Dohnanyi, J. S. 1969. Collisional model of asteroids and their debris. *J. Geophys. Res.* **74,** 2531–2554.

Dollfus, A., M. Wolff, J. E. Geake, D. F. Lupishko, and L. M. Dougherty 1989. Photopolarimetry of asteroids. In *Asteroids II* (R. P. Binzel *et al.,* Eds.), pp. 594–616. Univ. of Arizona Press, Tucson.

Drake, M. 1979. Geochemical evolution of the eucrite parent body: Possible nature and evolution of asteroid 4 Vesta? In *Asteroids* (T. Gehrels, Ed.), pp. 765–782. Univ. of Arizona Press, Tucson.

FARINELLA, P., CH. FROESCHLÉ, C. FROESCHLÉ, R. GONCZI, G. HAHN, A. MORBIDELLI, AND G. B. VALSECCHI 1994. Asteroids falling into the Sun. *Nature* **371,** 314–317.

FUJII, N., M. MIYAMOTO, Y. KOBAYASHI, AND K. ITO 1981. Differences of relative strength among chondrites measured by the vibrational fracturing rate. In *Proc. 6th Symp. Antarctic Meteorites,* 362–371.

FUJIWARA, A., T. KADONO, AND A. NAKAMURA 1993. Cratering experiments into curved surfaces and their implication for craters on small satellites. *Icarus* **105,** 345–350.

GAFFEY, M. J. 1983. The asteroid 4 Vesta: Rotational spectral variations, surface material homogeneity, and implications of the origins of the basaltic achondrites. *Lunar Planet Sci. Conf. XIV,* 231–232. [Abstract]

GAFFEY, M. J. 1995. Surface lithologic heterogeneity of asteroid 4 Vesta. *Icarus* submitted.

GARVIN, J. B. 1985. Blockfields on planetary surfaces. *Lunar Planet. Sci. Conf. XVI,* 260–261 [Abstract]

GAULT, D. E., AND E. D. HEITOWIT 1963. The partition of energy for hypervelocity impact craters formed in rock. *Proc. 6th Hypervelocity Impact Symp. 2,* 419–456.

GAULT, D. E., E. M. SHOEMAKER, AND H. T. MOORE 1963. *Spray Ejected from the Lunar Surface by Meteoroid Impact.* NASA TND-1767.

GEISSLER, P., J.-M. PETIT, AND R. GREENBERG 1994. Ida: Distribution and origin of surface blocks. *Lunar Planet. Sci. Conf. XXV,* 411–412. [Abstract]

GEISSLER, P., J.-M. PETIT, AND R. GREENBERG 1995. Ejecta reaccretion on rapidly rotating asteroids: Implications for 243 Ida and 433 Eros. *Proc. Astron. Soc. Pacific*, submitted.

GEISSLER, P., J.-M. PETIT, D. DURDA, R. GREENBERG, W. BOTTKE, M. NOLAN, AND J. MOORE 1996. Erosion and ejecta reaccretion on 243 Ida and its moon. *Icarus* **120,** 140–157.

GRATZ, A. J., W. J. NELLIS, AND N. A. HINSEY 1993. Observations of high-velocity, weakly shocked ejecta from experimental impacts. *Nature* **363,** 522–524.

GREELEY, R., R. SULLIVAN, R. PAPPALARDO, J. HEAD, J. VEVERKA, P. THOMAS, P. LEE, M. BELTON, AND C. CHAPMAN 1994. Morphology and geology of asteroid Ida: Preliminary Galielo imaging observations. *Lunar Planet. Sci. Conf. XXV,* 469–470. [Abstract]

GREENBERG, R., AND M. C. NOLAN 1989. Delivery of asteroids and meteorites to the inner solar system. In *Asteroids II*, (R. P. Binzel, T. Gehrels, and M. S. Matthews, Eds.), pp. 778–804. Univ. of Arizona Press, Tucson.

HAMANO, Y., AND K. YOMOGIDA 1982. Magnetic anisotropy and porosity of Antarctic chondrites. In *Proc. 7th Symp. Antarctic Meteorites,* 281–290.

HARTMANN, W. K. 1978. Planet formation: Mechanism of early growth. *Icarus* **33,** 50–61.

HEIKEN, G., D. VANIMAN, AND B. FRENCH 1991. *Lunar Sourcebook. A User's Guide to the Moon*, Cambridge Univ. Press, Cambridge, U.K.

HÖRZ, F., E. SCHNEIDER, D. E. GAULT, J. B. HARTUNG, AND D. BROWNLEE 1975. Catastrophic rupture of lunar rocks: A Monte Carlo simulation. *Moon* **13,** 235–258.

HÖRZ, F., AND R. B. SCHAAL 1981. Asteroidal agglutinate formation and implications for asteroidal surfaces. *Icarus* **46,** 337–353.

HOUSEN, K. R., L. L. WILKENING, C. R. CHAPMAN, AND R. GREENBERG 1979. Asteroidal regoliths. *Icarus* **39,** 317–351.

LEBOFSKY, L. A., AND G. H. RIEKE 1979. Thermal properties of 433 Eros. *Icarus* **40,** 297–308.

LEBOFSKY, L. A., AND J. R. SPENCER 1989. Radiometry and thermal modeling of asteroids. In *Asteroids II* (R. P. Binzel, T. Gehrels and M. S. Matthews, Eds.), pp. 128–147. Univ. of Arizona Press, Tucson.

LEE, P., J. VEVERKA, M. J. S. BELTON, P. C. THOMAS, B. T. CARCICH, R. GREELEY, R. SULLIVAN, R. PAPPALARDO, AND THE GALILEO SSI TEAM 1994. Mapping regolith and blocks on asteroid 243 Ida: The effects of photometric viewing geometry. *Lunar Planet. Sci. Conf. XXV,* 787–788. [Abstract]

LEE, S. W., P. THOMAS, AND J. VEVERKA 1986. Phobos, Deimos, and the Moon: Size and distribution of crater ejecta blocks. *Icarus* **68,** 77–86.

MCGETCHIN, T. R., M. SETTLE, AND J. W. HEAD 1973. Radial thickness variation in impact crater ejecta: Implications for lunar basin deposits. *Earth Planet. Sci. Lett.* **20,** 226–236.

MCKAY, D. S., T. D. SWINDLE, AND R. GREENBERG 1989. Asteroidal regoliths: What do we know? In *Asteroids II*, (R. Binzel, T. Gehrels, and M. S. Matthews, Eds.), pp. 617–642. Univ. of Arizona Press, Tucson.

MELOSH, H. J. 1984. Impact ejection, spallation, and the origin of meteorites. *Icarus* **59,** 234–260.

MELOSH, H. J. 1985. Ejection of rock fragments from planetary bodies. *Geology* **13,** 144–148.

MELOSH, H. J. 1989. *Impact Cratering: A Geologic Process.* Oxford Univ. Press, New York.

MELOSH, H. J., E. V. RYAN, AND E. ASPHAUG 1992. Dynamical fragmentation in impacts. *J. Geophys. Res.* **97,** 14735–14759.

MOORE, H. J. 1971. Large blocks around lunar craters. In *Analysis of Apollo 10 Photography and Visual Observations,* pp. 26–27. NASA SP-232, Washington, DC.

NAKAMURA, A., AND A. FUJIWARA 1991. Velocity distribution of fragments formed in simulated collisional disruption. *Icarus* **92,** 462–477.

NOLAN, M. C., E. ASPHAUG, AND R. GREENBERG 1992. Numerical simulations of regolith production on 951 Gaspra. *Meteoritics* **27,** 270–271. [Abstract]

REEDY, R. C., J. R. ARNOLD, AND D. LAL 1983. Cosmic-ray record in solar system matter. *Annu. Rev. Nucl. Part. Sci.* **33,** 505–537.

SCHMIDT, R. M., AND K. R. HOUSEN 1987. Some recent advances in the scaling of impact and explosion cratering. *Int. J. Impact Eng.* **5,** 543–560.

SCHULTZ, P. H. 1976. *Moon Morphology. Interpretations Based on Lunar Orbiter Photography.* Univ. of Texas Press, Austin and London.

SCHULTZ, P. H., AND W. MENDELL 1978. Orbital infrared observations of lunar craters and possible implications for impact ejecta emplacement. *Proc. Lunar Planet. Conf. 9th*, 2857–2883.

SCHULTZ, P. H., D. ORPHAL, B. MILLER, W. F. BORDEN, AND S. A. LARSON 1981. Multi-ring basin formation: Possible clues from impact cratering calculations. In *Multi-Ring Basins* (P. H. Schultz and R. B. Merrill, Eds.), Proc. Lunar Planet. Sci. (1981), 12A, 181–195.

SHOEMAKER, E. M., AND S. W. KIEFFER 1974. *Guidebook to the Geology of Meteor Crater, Arizona.* Publication No. 17. Center for Meteorite Studies, Arizona State University, Tempe, AZ.

SOTER, S. 1971. *The Dust Belts of Mars.* CRSR Report 462, Cornell University, Ithaca, NY.

STÖFFLER, D., A. BISCHOFF, V. BUCHWALD, AND A. E. RUBIN 1988. Shock effects in meteorites. In *Meteorites and the Early Solar System* (J. F. Kerridge and M. S. Matthews, Eds.), pp. 165–202. Univ. of Arizona Press, Tucson.

SULLIVAN, R., R. GREELEY, R. PAPPALARDO, E. ASPHAUG, J. MOORE, D. MORRISON, M. J. S. BELTON, M. CARR, C. R. CHAPMAN, P. GEISSLER, R. GREENBERG, J. GRANAHAN, J. W. HEAD III, R. KIRK, A. MCEWEN, P. LEE, P. C. THOMAS, J. VEVERKA 1996. Geology of 243 Ida. *Icarus* **120,** 119–139.

THOMAS, P. 1979. Surface features of Phobos and Deimos. *Icarus* **40,** 223–243.

THOMAS, P. 1993. Gravity, tides, and topography on small satellites and

asteroids: Application to surface features of the martian satellites. *Icarus* **105,** 326–344.

THOMAS, P. C., J. VEVERKA, A. BLOOM, AND T. DUXBURY 1979. Grooves on Phobos: Their distribution, morphology, and possible origin. *J. Geophys. Res.* **84,** 8457–8477.

VEVERKA J., AND P. THOMAS 1979. Phobos and Deimos: A preview of what asteroids are like? In *Asteroids* (T. Gehrels, Ed.), pp. 628–651. Univ. of Arizona Press, Tucson.

VEVERKA, J., M. BELTON, K. KLAASEN, AND C. CHAPMAN 1994a. Galileo's encounter with 951 Gaspra: Overview. *Icarus* **107,** 2–17.

VEVERKA, J., P. THOMAS, P. LEE, P. HELFENSTEIN, M. J. S. BELTON, C. CHAPMAN, K. KLAASEN, T. V. JOHNSON, A. HARCH, M. DAVIES, AND THE GALILEO IMAGING TEAM 1994b. Ida's satellite: What is it like? *Bull. Am. Astron. Soc.* **26,** 1155 [Abstract]

VEVERKA, J., P. C. THOMAS, P. HELFENSTEIN, P. LEE, A. HARCH, S. CALVO, C. CHAPMAN, M. J. S. BELTON, K. KLAASEN, T. V. JOHNSON, AND M. DAVIES 1996. Dactyl: Galileo observations of Ida's satellite. *Icarus* **120,** 200–211.

VICKERY, A. M. 1987. Variation in ejecta size with ejection velocity. *Geophys. Res. Lett.* **14,** 726–729.

WASSON, J. T. 1985. *Meteorites. Their Record of Early Solar-System History.* Freeman, New York.

WETHERILL, G. W. 1974. Solar system sources of meteorites and large meteoroids. *Ann. Rev. Earth Planet. Sci.* **2,** 303–331.